Unconventional quantum criticality in $YbRh_2Si_2$

P. Gegenwart[a,*], T. Westerkamp[b], C. Krellner[b], M. Brando[b], Y. Tokiwa[c], C. Geibel[b], F. Steglich[b]

[a] *I. Physikalisches Institut, Georg-August-Universität Göttingen, Friedrich-Hund-Platz 1, D-37077 Göttingen, Germany*
[b] *Max-Planck-Institute for Chemical Physics of Solids, D-01187 Dresden, Germany*
[c] *Los Alamos National Laboratory, Los Alamos, NM 87545, USA*

Abstract

$YbRh_2Si_2$ is a clean heavy fermion system which displays a magnetic field tuned quantum critical point. We present low-temperature electrical resistivity, magnetostriction and magnetization measurements on high-quality single crystals with a residual resistivity ratio of 150. The data provide evidence for a low-energy scale $T^\star(H)$ which vanishes in addition to the boundaries of the magnetic ordering and Landau Fermi liquid regime at the quantum critical point, indicating unconventional quantum criticality.

Keywords: $YbRh_2Si_2$; Quantum critical point; Non-Fermi liquid behavior

1. Introduction

The tetragonal $YbRh_2Si_2$ (YRS) is one of the few clean and stoichiometric heavy fermion (HF) systems that are located at ambient pressure and zero magnetic field extremely close to a quantum critical point (QCP) [1]. It shows an antiferromagnetic (AF) ordering at a very low Néel temperature of $T_N = 70\,\mathrm{mK}$ and a very small magnetic field of 0.05 T tunes its ground state across the QCP into the paramagnetic Landau Fermi liquid (LFL) regime [2]. In this paper, we focus on low-temperature thermodynamic, magnetic and transport measurements on YRS which hint at unconventional quantum criticality in this system.

The *conventional* theory for AF QCPs in HF systems considers itinerant f-electrons at both sides of the QCP. Their scattering off the critical spin-density-wave (SDW) fluctuations gives rise to non-Fermi liquid behavior [3–5]. Since singular scattering is restricted to certain "hot lines" at the Fermi surface (connected by the critical **Q**-vector of the nearby SDW), large parts of the Fermi surface remain "normal" for 3D critical fluctuations in this scenario, and the quasiparticle mass saturates in the approach of the QCP (for 2D critical fluctuations, the theory predicts a logarithmic mass divergence). Motivated by experiments on $CeCu_{6-x}Au_x$ [6], *unconventional* scenarios for quantum criticality in HF systems have been proposed [7–11]. They consider a localization of the f-electrons at the QCP. As a consequence, the Fermi surface volume shows a jump across the QCP. These ideas are supported by recent studies of the de Haas–van Alphen effect. Upon tuning AF systems like $CeRhIn_5$ by hydrostatic pressure through their QCPs drastic changes of the Fermi surface have been detected [12]. Since the Hall effect should be a sensitive probe of the evolution of the Fermi surface volume [7], results of this quantity on YRS are discussed below.

The high-temperature and high-magnetic field properties of YRS are summarized in Ref. [13]. The single-ion Kondo scale of the system amounts to 25 K. Magnetic fields larger than 10 T, applied along the easy direction perpendicular to the *c*-axis, are sufficient to the suppress HF behavior. The boundary of the very weak AF state is located well inside this regime: $T_N = 70\,\mathrm{mK}$ and the critical field $H_c \approx 0.05\,\mathrm{T}$ (for fields along the easy plane). Hydrostatic pressure increases T_N, as expected for Yb-systems, whereas a partial

*Corresponding author. Tel.: +49 551 397607; fax: +49 551 3919546.
E-mail address: pgegenw@gwdg.de (P. Gegenwart).

substitution of Si by the isoelectronic but larger Ge reduces T_N to 20 mK in $YbRh_2(Si_{0.95}Ge_{0.05})_2$ [14]. For the latter system, a detailed thermodynamic analysis close to the QCP has been performed: a stronger than logarithmic mass divergence [14] as well as fractional exponent in the divergence of the Grüneisen ratio [15] exclude the conventional description of quantum criticality in YRS.

Very recently it has been proposed that the weak AF ordering in YRS may result from a minor (few percent) volume fraction of Yb^{3+} ions with a very low single-ion Kondo temperature [16]. However, clear phase transition anomalies observed e.g. in specific heat [14] or thermal expansion [17] provide evidence for the bulk nature of the transition. Furthermore, a continuous increase of T_N and the entropy $S(T_N)$ is observed under hydrostatic pressure [18,19] which could hardly be explained within such an impurity scenario. Also, Ge-doping on the Si-site [14], as well as La-doping on the Yb-site [20] lead to a suppression of T_N that is consistent with the effect of the volume expansion but inconsistent with the impurity scenario. Further on, there is no indication that T_N depends on the residual resistivity of the studied YRS single crystals, which itself would be very sensitive to Yb^{3+} ions with very low T_K. In fact previous studies have been done on single crystals with a residual resistivity ratio (RRR) of 25 [1] and the newest generation exhibit a RRR up to 150, i.e. $\rho_0 \approx 0.5\,\mu\Omega\,cm$.

The Hall effect evolution across the QCP has been studied in great detail [21]. Most remarkably, the suppression of the tiny magnetic ordering with an ordered moment of about $10^{-3}\mu_B$/Yb [22] by magnetic field leads to a large (about 30%) change of the Hall coefficient. A new line in the temperature-field phase diagram has been discovered across which the isothermal Hall-resistivity as a function of the applied magnetic field changes. Upon decreasing the temperature this feature sharpens, suggesting for the zero-temperature extrapolation a sudden change of the Fermi surface at the QCP [21]. In the following, we will study the evolution of the low-temperature electrical resistivity, magnetostriction and magnetization on high-quality single crystals upon passing this "Hall-line".

2. Electrical resistivity

Fig. 1 shows low-temperature resistivity data of a high-quality YRS single crystal. At zero field a sharp anomaly marks the onset of AF ordering. Upon application of small magnetic fields perpendicular to the c-axis, T_N is continuously suppressed towards zero at the critical field $H_c = 0.05$ T. At $H > H_c$, the low-temperature resistivity follows $\Delta\rho = A(H)T^2$ for temperatures below $T_{LFL}(H)$. Approaching the critical field, $T_{LFL} \to 0$ and $A \to \infty$ (see also Ref. [2] for a study on a single crystal with $\rho_0 = 1\,\mu\Omega\,cm$). At the critical field, the resistivity shows a linear temperature dependence down to the lowest measured temperature of 20 mK (cf. red curve in Fig. 1). This is in contrast to the reported T^2 behavior even directly at the

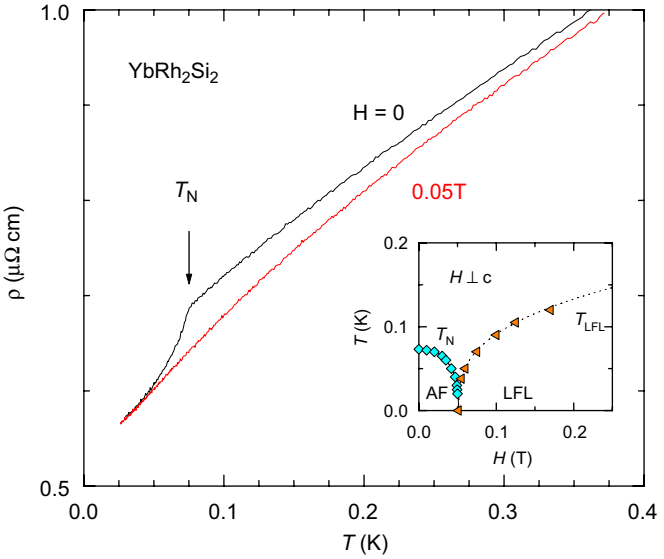

Fig. 1. Low-temperature electrical resistivity of high-quality $YbRh_2Si_2$ single crystal at $H = 0$ and 0.05 T (applied perpendicular to the c-axis). The inset shows the temperature-field phase diagram determined from measurements of the same sample at various magnetic fields. The boundaries of the antiferromagnetically ordered (AF) and Landau Fermi liquid (LFL) regime have been determined from the position of a kink in $\rho(T)$ (cf. arrow in main part of Fig. 1) and upper limit of T^2 behavior, respectively.

critical field in Ref. [19]. We stress that our observation of a linear resistivity dependence at $H = H_c$ down to 20 mK has been reproduced on different single crystals [2]. Deviations from $\Delta\rho \propto T$ could either result from heating effects at the contacts, a field inhomogeneity, or from a non-precise determination of the critical field value. Since the boundaries of the AF and LFL states in the phase diagram are very steep (cf. inset of Fig. 1), a linear resistivity can only be obtained for a very precise tuning of the applied field. Complementary measurements of the low-temperature specific heat on a crystal of the same batch have revealed a power-law divergence of $C(T)/T$ at $H = H_c$, with similar exponent as observed previously for Ge-doped YRS [23]. This proves the stronger than logarithmic mass divergence at the QCP in this system.

We now turn to measurements of the isothermal magnetoresistance (Fig. 2). The maximum for $T < T_N$ marks the boundary of the AF state. At $T > T_N$ an additional signature is observed. The arrows indicate inflection points, whose positions are marked by the yellow triangles in the phase diagram shown in the inset. As will be discussed in the following, these positions agree with the line of anomalies in the Hall-effect, magnetostriction and magnetization.

3. Magnetostriction

Measurements on the isothermal magnetostriction ($H \perp c$) have been performed using an ultrahigh resolution capacitive dilatometer on a high-quality (RRR = 150)

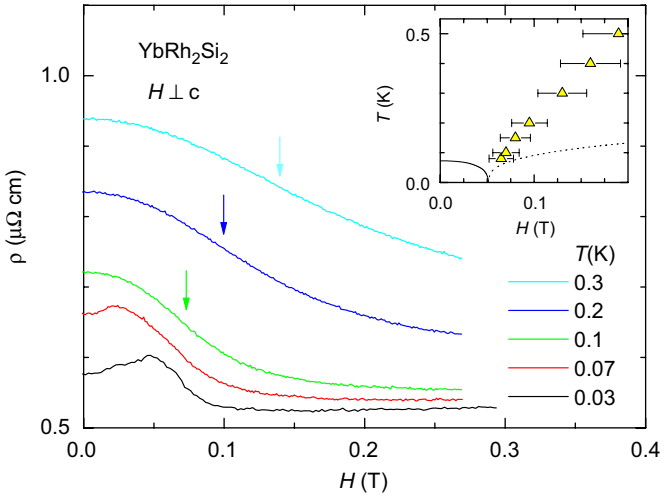

Fig. 2. Longitudinal magnetoresistivity of $YbRh_2Si_2$ as ρ vs H ($H \perp c$) at various temperatures. The maxima in the 0.03 and 0.07 K data indicate the boundary of the AF state. The arrows mark the positions of the inflection points in $\rho(H)$ as determined from minima in $d\rho/dH$ [24]. The inset displays the phase diagram, where the solid and dotted lines represent the boundaries of the AF and LFL state. Open yellow triangles mark the positions of the inflection points with H.

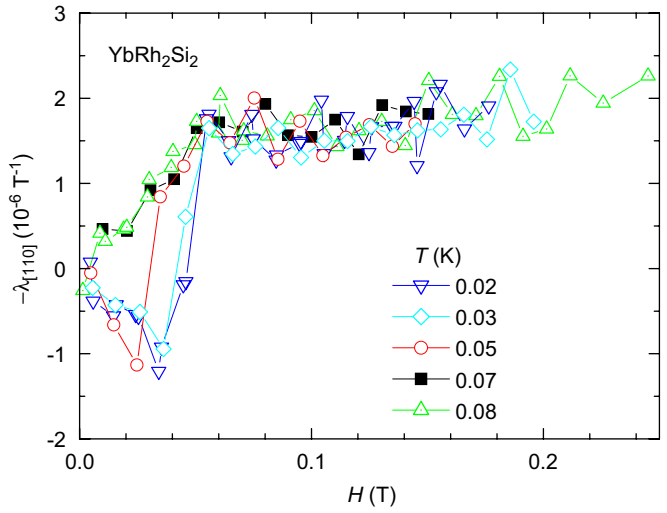

Fig. 3. Isothermal magnetostriction coefficient $\lambda = \partial \ln L/\partial H$ (where L is the sample length along the [1 1 0] direction) of $YbRh_2Si_2$ as $-\lambda$ vs H at temperatures between 0.02 and 0.08 K.

single crystal. The magnetostriction coefficient $\lambda_{[1\,1\,0]} = L^{-1}\,dL/dH$ with the sample length L along the [1 1 0] direction has been determined by calculating the field derivative of the length change over intervals of 5–20 mT. At very low temperatures, as shown in Fig. 3, the suppression of AF ordering at $H_c = 0.05$ T results in a steplike change of λ, as expected for a second-order phase transition. Upon increasing T, this anomaly shifts towards lower field values and vanishes for temperatures above T_N. However, instead of showing a smooth behavior at $T > T_N$, a kink-like structure is observed, which broadens and shifts towards higher fields with increasing temperature

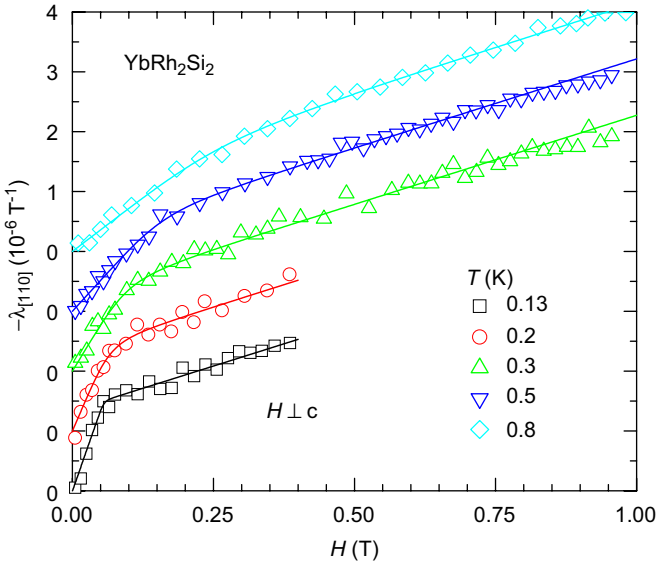

Fig. 4. Isothermal magnetostriction as in Fig. 3 for temperatures between 0.13 and 0.8 K. The data sets have been shifted by different amounts vertically. The solid lines are fits using the integral of the crossover function $f(H, T)$, see text.

(see Fig. 4). For usual metals, a linear field dependence of the magnetostriction coefficient is observed [25]. The observed magnetostriction behavior may thus be interpreted as a signature of a change between different metallic states.

In order to extract an energy scale $T^\star$ from the anomalies, we have fitted the data to the integral of the crossover function $f(H,T) = A_2 - (A_2 - A_1)/[1 + (H/H_0)^p]$ (cf. Ref. [21]) which reveals a characteristic field H_0 along which the magnetostriction shows a drastic change in slope [24]. As will be shown later, the positions $H_0(T)$ agree well with the respective anomalies in the Hall effect [21], magnetization, susceptibility as well as longitudinal resistivity, establishing the existence of an intrinsic energy scale $T^\star(H)$ which vanishes at the QCP.

4. Magnetization

It has been shown previously [1,26] that the magnetic susceptibility $\chi(T)$ shows characteristic maxima in the temperature dependence at $H > H_c$. This signature results from a strongly nonlinear low-temperature magnetization behavior $M(H)$ which is smeared out with increasing temperature [27]. Fig. 5 displays $M(H)$ for a high-quality (RRR = 150) single crystal which strongly resembles the change of the magnetostriction coefficient discussed in the previous section. In order to extract the crossover field H_0, we have analyzed $\tilde{M} \equiv M + \chi H$, which is the field derivative of the magnetic free energy contribution $(-M \times H)$ [24]. The magnetization itself shows a similar crossover as $M + \chi H$ does, cf. Fig. 5. Compared to the $\tilde{M}$ case, its linear H dependence in the measured high-field regime is somewhat less robust, making the fit by the function $f(H, T)$ to be of a slightly lower quality [24].

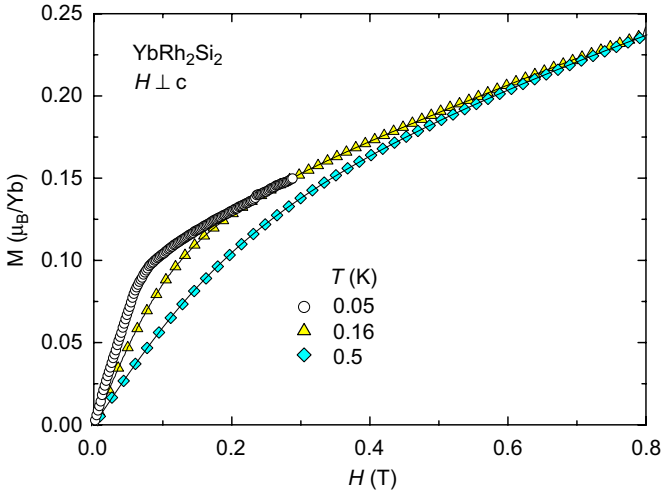

Fig. 5. Isothermal magnetization of $YbRh_2Si_2$ with H perpendicular to the c-axis.

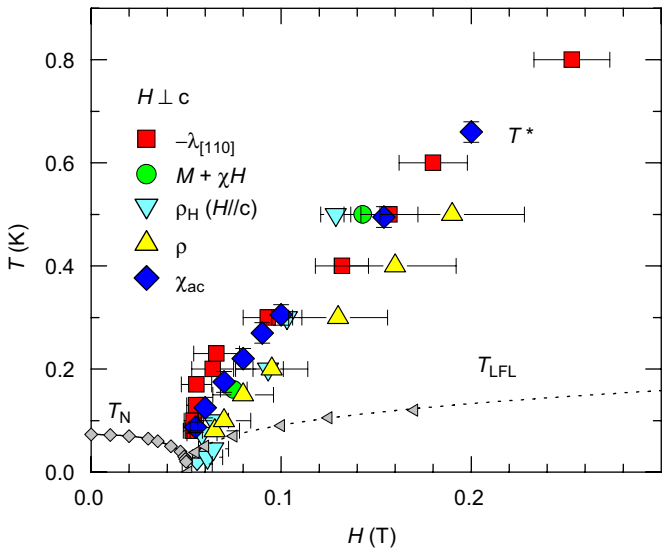

Fig. 6. Temperature vs magnetic field phase diagram for $YbRh_2Si_2$ ($H \perp c$). The gray diamonds and triangles denote the boundaries of the AF and LFL regime, respectively, and have been determined from electrical resistivity measurements on a high-quality (RRR = 150) single crystal. Colored symbols mark $T^\star(H)$ as determined from magnetostriction (λ), magnetization ($\tilde{M}$), Hall resistivity (ρ_H for $H \| c$ [21]; the field values have been divided by an anisotropy factor 13.2), longitudinal resistivity (ρ), as well as ac-susceptibility (χ_{ac}).

The causal relationship between the observed magnetization signature and the Hall effect change has been discussed in Ref. [24]. For $H \perp c$ the "kink-like" signature in $M(H)$ is too weak to explain the smeared jump as a function of the tuning field (parallel to the current direction) in the Hall coefficient [21]. For $H \| c$, the magnetization is almost linear [27]. Thus, it is natural to view the magnetization and magnetostriction anomalies as thermodynamic signatures of the same change of the Fermi surface volume indicated by the Hall data.

5. Phase diagram

We have shown previously, that $\tilde{M}(H)$, $\lambda(H)$, and the Hall resistivity $\rho_H(H)$ (measurements for $H \| c$, which have been scaled by the anisotropy ratio 13.2) all show similar crossovers, which can be described by the integral of the function $f(H,T)$ [24]. In the limit $T \to 0$ and for all different properties the full-width at half-maximum and the ratio A_2/A_1 extrapolate to zero and a value different from 1, respectively (cf. supplementary information to Ref. [24]). This indicates that the differentials of each quantity exhibit a jump across the QCP.

The positions of the crossovers observed in the various measurements [24] are summarized in Fig. 6. The data establish a thermodynamic energy scale $T^\star$ that vanishes at the magnetic field tuned QCP in YRS.

6. Conclusion

The conventional theory for quantum criticality is based on an itinerant description in which magnetic-order parameter fluctuations in spatial and temporal dimensions are considered only [3–5]. This theory predicts a phase diagram with a boundary of LFL behavior that vanishes at the QCP. Our results on YRS prove the existence of an *additional* energy scale $T^\star(H)$ vanishing at the QCP, too. The comparison with Hall-effect measurements [21] indicates that this scale is a finite-T manifestation of the localization of the f-electrons at the QCP [24]. Our results thus prove that magnetic slowing-down near the QCP can be accompanied by an additional slowing down, i.e. an electronic one, due to the f-localization. A description based solely on magnetic order parameter fluctuations is then insufficient and *unconventional* scenarios are needed. To date there exist different proposals which are based either upon a complete [7–9] or partial [11] breakdown of the Kondo effect at the QCP or upon the extension of "deconfined quantum criticality" in quantum magnets to the case of HF systems [10].

The interesting question arises whether the magnetic QCP can be separated from the f-localization transition. We plan to investigate the evolution of $T_N(H)$, $T^\star(H)$ and $T_{LFL}(H)$ as a function of small changes of the unit cell volume. Such studies could be done on $Yb(Rh_{1-x}M_x)_2Si_2$ (M = Ir, Co), in which a fraction of Rh-atoms is substituted isoelectronically by either larger Ir- or smaller Co-atoms [28].

Acknowledgments

We gratefully acknowledge conversations with E. Abrahams, P. Coleman, J. Custers, S. Friedemann, N. Oeschler, S. Paschen and Q. Si.

References

[1] O. Trovarelli, et al., Phys. Rev. Lett. 85 (2000) 626.
[2] P. Gegenwart, et al., Phys. Rev. Lett. 89 (2002) 056402.

[3] J.A. Hertz, Phys. Rev. B 14 (1976) 1165.
[4] A.J. Millis, Phys. Rev. B 48 (1993) 7183.
[5] T. Moriya, T. Takimoto, J. Phys. Soc. Japan 64 (1995) 960.
[6] A. Schröder, et al., Nature 407 (2000) 351.
[7] P. Coleman, C. Pépin, Q. Si, R. Ramazashvili, J. Phys. Condens. Matter 13 (2001) R723.
[8] Q. Si, S. Rabello, K. Ingersent, J.L. Smith, Nature 413 (2001) 804.
[9] I. Paul, C. Pépin, M.R. Norman, Phys. Rev. Lett. 98 (2007) 026402.
[10] T. Senthil, S. Sachdev, M. Vojta, Physica B 359–361 (2005) 9.
[11] H. Watanabe, M. Ogata, Physica B (2007), doi:10.1016/j.physb.2007.10.141.
[12] H. Shishido, R. Settai, H. Harima, Y. Onuki, J. Phys. Soc. Japan 74 (2005) 1103.
[13] P. Gegenwart, et al., New J. Phys. 8 (2006) 171.
[14] J. Custers, et al., Nature 424 (2003) 524.
[15] R. Küchler, et al., Phys. Rev. Lett. 91 (2003) 066405.
[16] Z. Fisk, et al., these proceedings.
[17] R. Küchler, et al., J. Magn. Magn. Mater. 272–276 (2004) 229.
[18] S. Mederle, et al., J. Phys. Condens. Matter 14 (2002) 10731.
[19] G. Knebel, et al., J. Phys. Soc. Japan 75 (2006) 114709.
[20] J. Ferstl, et al., Physica B 359–361 (2005) 26.
[21] S. Paschen, et al., Nature 432 (2004) 881.
[22] K. Ishida, et al., Phys. Rev. B 68 (2003) 184401.
[23] N. Oeschler, et al., Physica B (2007), doi:10.1016/j.physb.2007.10.119.
[24] P. Gegenwart, et al., Science 315 (2007) 969.
[25] B.S. Chandrasekhar, E. Fawcett, Adv. Phys. 20 (1971) 775.
[26] P. Gegenwart, J. Custers, Y. Tokiwa, C. Geibel, F. Steglich, Phys. Rev. Lett. 94 (2005) 076402.
[27] P. Gegenwart, Y. Tokiwa, J. Custers, C. Geibel, F. Steglich, J. Phys. Soc. Japan 75 (Suppl) (2006) 155.
[28] T. Westerkamp, et al., Physica B (2007), doi:10.1016/j.physb.2007.10.114.